

Coefficient of restitution for wet particles

Frank Gollwitzer, Ingo Rehberg, and Kai Huang*
Experimentalphysik V, Universität Bayreuth, 95440 Bayreuth, Germany

Christof A. Kruehle
Maschinenbau und Mechatronik, Hochschule Karlsruhe - Technik und Wirtschaft, D-76133 Karlsruhe, Germany
 (Dated: February 9, 2012)

The influence of a wetting liquid on the coefficient of restitution (COR) is investigated experimentally by tracing freely falling particles bouncing on a wet surface. The dependence of the COR on the impact velocity and various properties of the particle and the wetting liquid is presented and discussed in terms of dimensionless numbers that characterize the interplay between inertial, viscous, and surface forces. In the Reynolds number regime where the lubrication theory does not apply, the ratio of the film thickness to the particle size is found to be a crucial parameter determining the COR.

PACS numbers: 45.70.-n, 45.50.Tn, 47.55.Kf

I. INTRODUCTION

The coefficient of restitution (COR), first introduced by Newton [1] as the ratio between the relative rebound and impact velocities of a binary impact, has been a subject of continuous interest over centuries, along with the development of elastic [2, 3], viscoelastic [4] and plastic theories [5, 6]. It characterizes the energy dissipation associated with the impact, which plays a key role in understanding the collective behavior of macroscopic particles, i.e. the dynamics of granular matter [7, 8]. This is largely due to the fact that the dissipative nature of granular matter arises from the inelastic collisions at the particle level.

Due to its omnipresence in nature and various industries, granular matter has drawn great attention from both physical and engineering communities in the past decades [9]. Concerning the modeling of granular matter, an appropriate collision model is essential for the successful implementation of kinetic or hydrodynamic theories to granular matter [10–13], see for example the dynamics of Saturn’s rings [14], or the pattern formation under vertical agitation [15]. Despite those successful examples for dry granular matter, a continuum description for wet granular matter, which considers the cohesion arising from the wetting liquid phase, is still far from established [16, 17]. Therefore, in order to provide a solid basis for a continuum modeling of wet granular flow – for example to describe natural disasters such as debris flow – a thorough understanding of the dynamics associated with wet impacts is desirable.

With the development of pharmaceuticals, mining and food industries, the COR for wet impacts has become an important issue for the engineering community in terms of decoding the underlying physics associated with the agglomeration of particles with liquid binders. The pi-

oneering work by Rumpf [18] half a century ago has included a detailed description of the capillary force of a pendular bridge and treated it as the dominating cohesive force in determining the statical behavior of wet granular matter, e.g. the tensile strength [19]. Later on, the viscous force has been found to play an important role in typical granulation processes, too [20–27]. And a dynamic liquid bridge could be an order of magnitude stronger than a quasi-static one [28, 29]. Binary impacts of particles with viscous liquid coating have been extensively investigated by experiments and models using lubrication theory [30–34].

Recently, a new class of collision experiments investigating three-body interactions utilizing a “Stokes’s Cradle” apparatus, revealed a more complex scenario [35, 36]: In addition to the agglomerated and separated final states known from binary impacts, partially sepa-

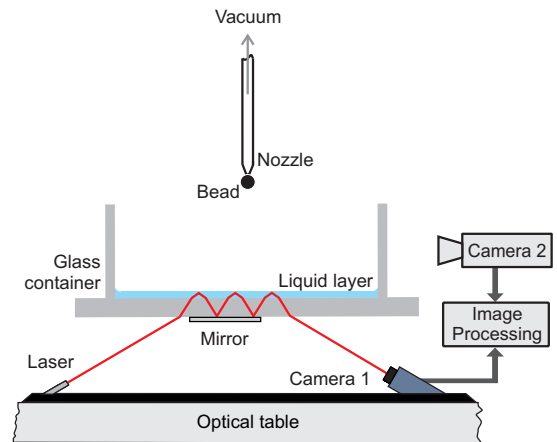


FIG. 1. (color online) Sketch of the experimental setup. The bouncing of the glass bead, initially held by the vacuum nozzle, on the glass container is recorded with a high speed camera (Camera 2). The thickness of the liquid layer is monitored by detecting the laser beam (red line) reflected from the liquid surface with Camera 1.

* kai.huang@uni-bayreuth.de

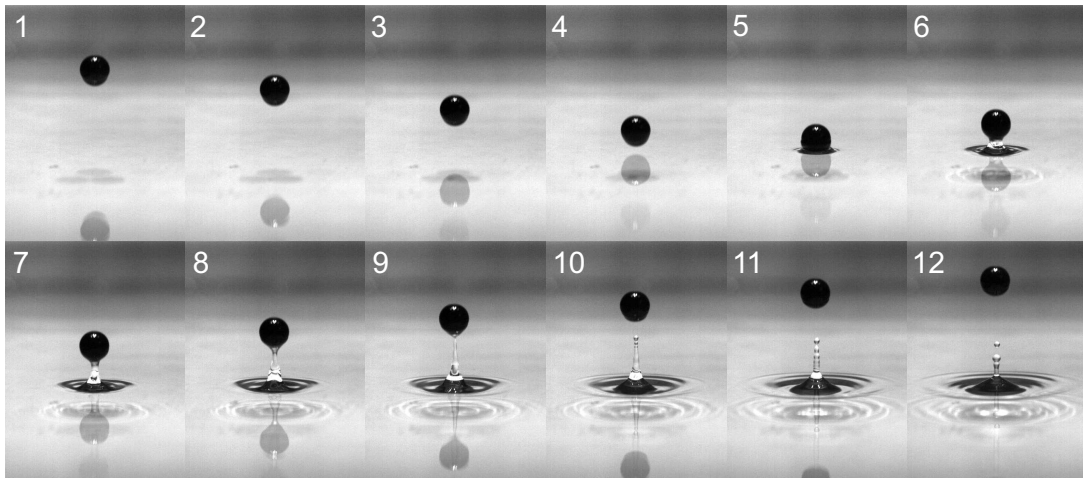


FIG. 2. A series of snapshots captured with a frame rate of 450 Hz showing a 4 mm glass bead bouncing on a glass plate covered with a 1 mm water film.

rated outcomes including a “Newton’s cradle” and a “reverse Newton’s cradle” collision could be observed.

Despite all those investigations, a well tested collision law suitable for modeling the dynamics of wet granular behavior [37–39], as well as a comprehensive knowledge of the energy dissipation associated with the impact, is still lacking. In the current work, the COR of a ball bouncing back from a flat lubricated surface is investigated as a function of the impact velocity and various particle as well as liquid properties. From this, the kinetic energy dissipated during the impact process is derived and discussed within the framework of existing models.

II. EXPERIMENTAL SETUP AND PROCEDURE

Figure 1 shows a sketch of the experimental setup used for the COR measurements. Spherical glass beads (SiLiBeads type P) with a diameter range from $D = 2.8$ mm to 10 mm, roughness $\approx 5 \mu\text{m}$, and density $\rho_g = 2.58 \text{ g/cm}^3$ are used in the experiments. By controlling the pressure in the vacuum nozzle, the initially wet particle is released from its starting position and falls onto a glass container ($20 \text{ cm} \times 5 \text{ cm}$) covered with a thin layer of wetting liquid: Purified water or silicone oil (Carl Roth M5 and M50) with dynamic viscosity η of 4.6 mPa s and 48 mPa s, respectively. The bottom of the container is 2 cm thick. It is leveled within 0.03 degrees, so that bouncing on various positions in the container explores a similar liquid layer thickness. The layer thickness δ is measured by detecting the shift of a laser beam reflected from the surface of the liquid and the glass plate with a CCD camera (Camera 1, Lumenera Lu135). The mirror attached to the bottom of the container creates multiple reflections of the laser beam, in order to enhance the sensitivity of the device. The length of the mirror (7.8 cm) is chosen as a compromise between the sensitivity and

the field of view. By fixing the container, laser and the camera on a leveled optical table, the error of the film thickness measurement could be minimized to a satisfactory level ($< 10 \mu\text{m}$).

To obtain the impact and rebound velocities, the bouncing of the particle is recorded by a fast camera (Photron Fastcam Super 10K) with succeeding digital image processing of individual frames. A close view of the colliding event, as shown in Fig. 2, clearly demonstrates the important role that the wetting liquid plays during the impact. As the sphere hits the liquid surface, a circular wave front occasionally accompanied with a splash will be generated. As the ball rebounds from the surface, a liquid bridge will form between the sphere and the liquid surface, which continuously deforms and elongates until it ruptures at a distance larger than the particle diameter. Associated with the rupture event, satellite droplets may form, which bounce on the liquid surface and coalesce partially into smaller droplets [40, 41]. Obviously, the formation of wave fronts, deformation and rupture of liquid bridges, the viscous force, and the added mass to the sphere due to the wetting liquid will all contribute to the mechanical energy reduction of the impacting particle, which in turn leads to a smaller COR compared with dry impacts.

Figure 3 illustrates the influence of wetting by providing a comparison between the trajectories obtained from wet and dry impacts. The particle diameter is $D = 5.5$ mm, and the film thickness of the silicone oil M5 is $\delta = 225 \mu\text{m}$ in the wet case. To determine the center of the sphere, the image processing procedure employs a Hough transformation [42] (upper panel of Fig. 3). Subsequently, each bouncing trajectory is extracted and subjected to a parabolic fit (see the solid line in Fig. 3(a) as an example), in order to obtain the peak position h_{peak} and the impact velocity. If the normal COR (e_n) is independent on the impact velocity, the velocity after the i th rebound will be related to the first impact velocity v_0 by

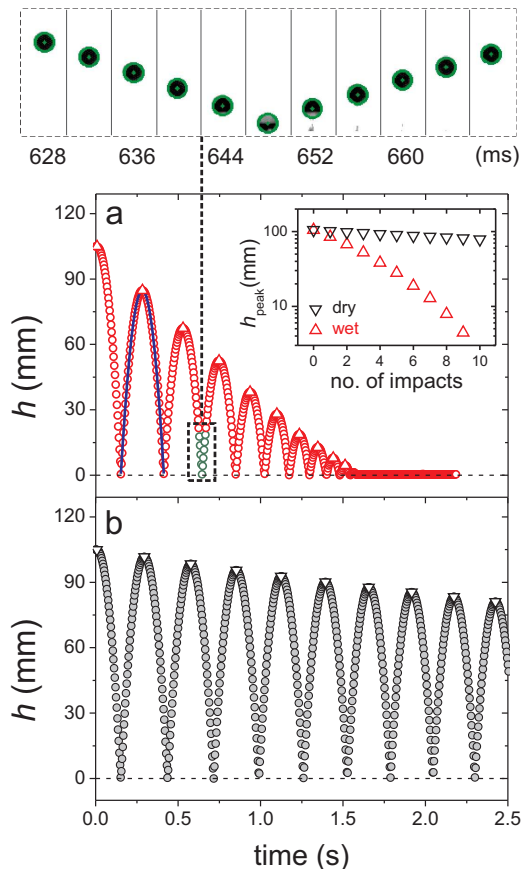


FIG. 3. (color online) Trajectories of a particle bouncing on a wet (a) and a dry (b) surface after image processing. The image sequence in the upper panel represents a fraction of the wet trajectory (a) with superimposed centers and boundaries of the sphere. The blue line in (a) corresponds to a parabolic fit to the trajectory after the first rebound. The peak positions of the trajectories h_{peak} obtained from the fits are marked with triangles in (a) and upside down triangles in (b). The inset in (a) shows h_{peak} as a function of the number of impacts.

$v_i = e_n^i v_0$. This leads to a linear decay of the peak height h_{peak} with the number of impacts i in a semi-log plot, according to $\lg h_{\text{peak}} = \lg h_0 + 2i \lg e_n$, with $h_{\text{peak}} \propto v_i^2$. The initial falling height h_0 and e_n determine the offset and slope of this line. As shown in the inset of Fig. 3(a), the logarithm of h_{peak} decreases linearly with the number of impacts for dry impacts, indicating that the normal COR stays almost constant for the number of impacts measured here. In a recent work on dry impacts [43], a more detailed analysis reveals that the dry COR decreases slightly with the increase of v_{impact} . However, this dependence is much weaker than the one for wet impacts, on which we are focusing here. In this case, the variation of the slope indicates that the COR for wet impacts decreases strongly with the number of impacts, i.e. with the impact velocity.

III. EXPERIMENTAL RESULTS

As shown in Fig. 4, this dependence of the COR on the impact velocity v_{impact} is qualitatively the same for various particle diameters and for both silicone oil (M5) and water wetting: It grows initially with v_{impact} and saturates at a certain value varying from 0.8 to 0.9. For a fixed v_{impact} , the COR decreases systematically with particle diameter for both silicone oil and water wetting. The monotonic growth of the COR on D reveals that the influence of the wetting liquid decreases as the inertia of the particle ($\propto D^3$) increases. In the lower panel of Fig. 4, the rebound velocity v_{rebound} is plotted as a function the impact velocity v_{impact} . Similar to the case without wetting liquid (shown as a gray dashed line), v_{rebound} grows linearly with v_{impact} , and the trend is qualitatively the same for all parameters used here. Therefore, fitting the data with $v_{\text{rebound}} = e_{\text{inf}}(v_{\text{impact}} - v_c)$ gives rise to two parameters that characterize the impact velocity dependence: A slope e_{inf} corresponding to the COR at infinite v_{impact} , i.e. the saturated value of the COR, and an offset v_c corresponding to a critical energy E_c below which no rebound would occur. $E_c = mv_c^2/2$ is obtained from the intersection v_c of the linear fits shown in the lower panels of Fig. 4 with the x-axis, where m is the mass of the particle.

Figure 5 shows the corresponding results. For the dry impacts, the results stem from linear fits of the data obtained for different particle sizes. The critical energy for the dry impacts is very close to 0. In contrast, the critical energy for wet impacts is on the order of few μJ . It shows a monotonic decay for water wetting, and a more complicated relationship for M5. As shown in Fig. 5 (b), e_{inf} – the upper limit of the COR – varies from 0.8 to 0.9, and is generally smaller than e_{dry} . From the energy dissipation perspective, this demonstrates that the ratio between the energy dissipation from the wetting liquid, ΔE_{wet} , and the kinetic energy at impact E_{impact} will not diminish as v_{impact} grows. For both silicone oil (M5) and water wetting, e_{inf} shows similar values with weak dependence on the particle sizes, although M5 silicone oil is 5 times more viscous than water.

The above experimental results indicate that the COR depends strongly on the impact velocity as well as various particle and liquid properties. In order to explore the relation between COR and all these parameters, it is essential to have a proper classification of the parameters in terms of dimensionless quantities that characterize the relation between inertia, viscous and capillary effects. In the case where the viscous force dominates, the dynamics of wet impacts could be described by the elastohydrodynamic theory [21, 30, 33, 36]. Within this framework, the Stokes number, defined as $St = \rho_g D v_{\text{impact}} / 9\eta$, is usually used to characterize the ratio between the inertia of the particle and the viscous force. Normally, this case is justified by the criterion that the Reynolds number of the wetting liquid $Re \ll 1$ [33], where $Re = \rho_l \delta v_{\text{impact}} / \eta$, with ρ_l the density and δ the thickness of the wetting liquid.

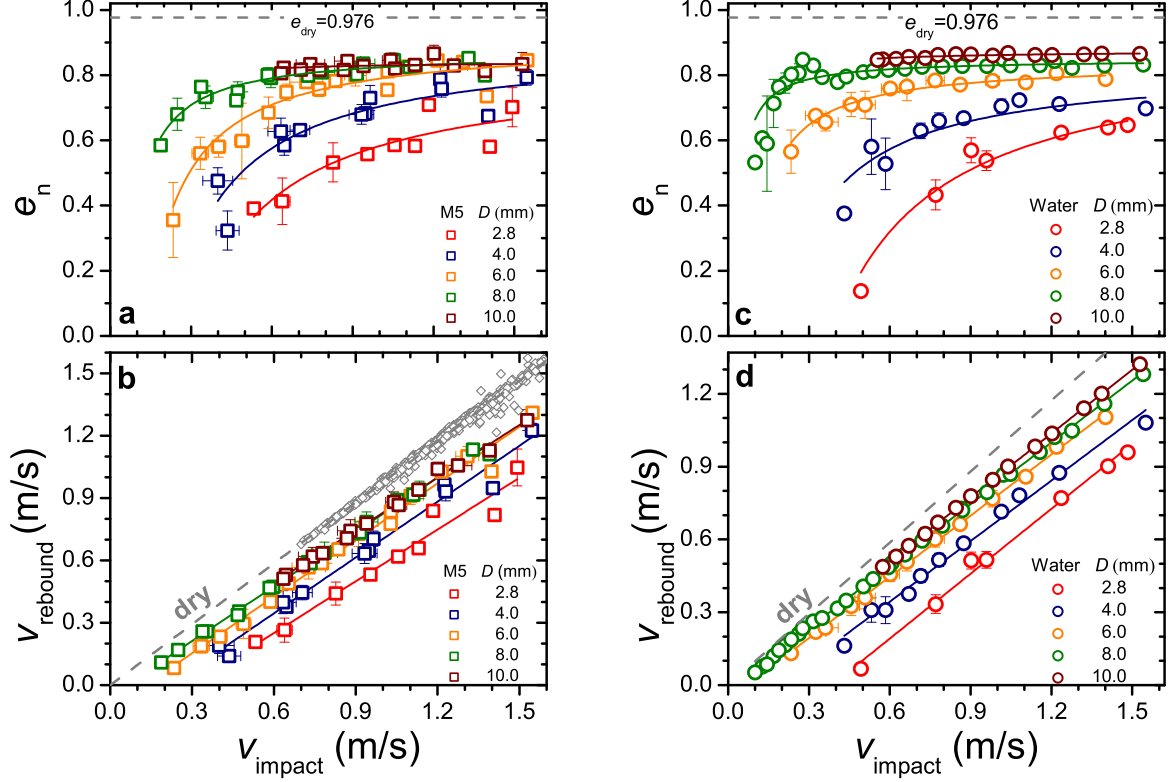


FIG. 4. (color online) Normal restitution coefficient e_n and rebound velocity v_{rebound} as a function of impact velocity v_{impact} for the impacts of particles with various diameters D on silicone oil (left column) and water (right column) wetting surfaces with fixed film thickness $\delta = 1$ mm. The solid lines in the lower panels are linear fits to the data and their representatives are shown in the upper panels as a guide to the eyes. The dashed gray lines in the upper panels represent the normal restitution coefficient $e_{\text{dry}} = 0.976 \pm 0.001$ for dry impacts, which is obtained by a linear fit of the data for all particle sizes (gray diamonds shown in b). Error bars smaller than the symbol size are not shown.

uid. This implies the conditions that either the liquid is highly viscous, or the film thickness is small enough for the lubrication theory to apply. Within this limit, the contribution from the wetting liquid to the total energy dissipation is mainly due to viscous damping. Although the range of Reynolds numbers for the current investigation ($10 < Re < 10^3$) suggests that the role that the viscous force plays may not be prominent, we represent the COR results shown in Fig. 4 with respect to the Stokes number as a starting point.

As shown in Fig. 6, the scaling of e_n with v_{impact} and D for more viscous silicone oil (M5) could be better described by the Stokes number St than that for water. For M5 wetting (corresponding to $Re = 20 - 360$), data for various D show a general trend of initial growth from $St \approx 100$ to 500, followed by a saturation to e_{inf} between 0.8 and 0.85. Concerning the case of water wetting (corresponding to $Re = 100 - 1800$), the scatter of the data obtained with various particle sizes (shown in Fig. 6(b)) is much more prominent than for the case of M5 wetting. Although the trend of a significant growth followed by a saturated value persists, both the slope of increase and

the saturated value differ as D varies. This difference between wetting liquids with various viscosity suggests that further parameters have to be considered as the Reynolds number goes beyond the regime where the elastohydrodynamic theory applies.

From another point of view, Fig. 6 also reveals a relatively small difference of the COR between M5 and water wetting, even though the corresponding viscosity ratio is 5. This result clearly demonstrates that the COR is also determined by other liquid properties. As an example, the surface tension of water ($\gamma = 72.0$ mN/m) is much larger than that of M5 (19.2 mN/m), which may lead to a larger energy dissipation from the formation of capillary waves and the break of capillary bridges upon rebound. To focus on the effect from viscosity, we use wetting liquids with similar surface tensions for comparison in the following part of the paper.

The influence of the liquid film thickness δ and the dynamic viscosity η on the wet impacts is presented in Fig. 7. The upper part (a) shows the corresponding normal restitution coefficient $e_n = v_{\text{rebound}}/v_{\text{impact}}$ as a function of v_{impact} . For wet impacts, e_n shows clearly a de-

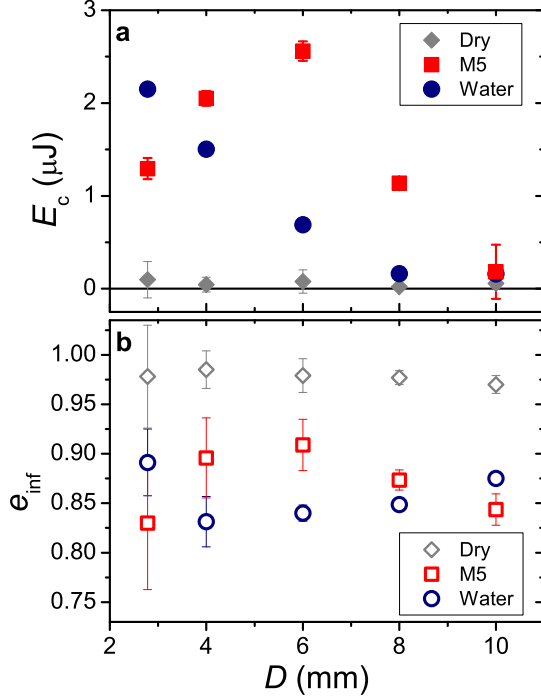


FIG. 5. The critical energy E_c and the saturated value of the COR e_{inf} as a function of particle diameter D . The solid line at $E_c = 0$ is a guide to the eyes.

pendence on v_{impact} , and this dependence is more prominent for a liquid film with higher viscosity. With M5 as wetting liquid, e_n grows slightly with v_{impact} and tends to saturate at a value depending on the film thickness δ . Similar to the results shown in Fig. 4, this value is smaller than e_{dry} , revealing the extra energy dissipation from the wetting liquid. As the film thickness δ increases, e_n decreases systematically for both wetting liquids, because the viscous damping force is effective over a larger distance. A comparison between the influence from the viscosity and the film thickness indicates that the former has a stronger impact on the energy dissipation and e_n .

In Fig. 7(b), the relation between v_{rebound} and v_{impact} is presented. For dry impacts, a linear growth of the rebound velocity v_{rebound} with the impact velocity v_{impact} without an offset suggests a constant $e_{\text{dry}} = 0.985$ for the range of v_{impact} explored here. For wet impacts, v_{rebound} decreases systematically with the liquid film thickness δ at a certain v_{impact} . As the liquid viscosity increases by an order of magnitude (from M5 to M50), this trend is more prominent, indicating the crucial role played by the viscous damping. The growth of v_{rebound} with v_{impact} could well be fitted with a straight line. The fit again gives rise to a slope e_{inf} that is smaller than e_{dry} and a threshold energy E_c below which no rebound would occur. As shown in Fig. 8(a), this threshold is, for M50,

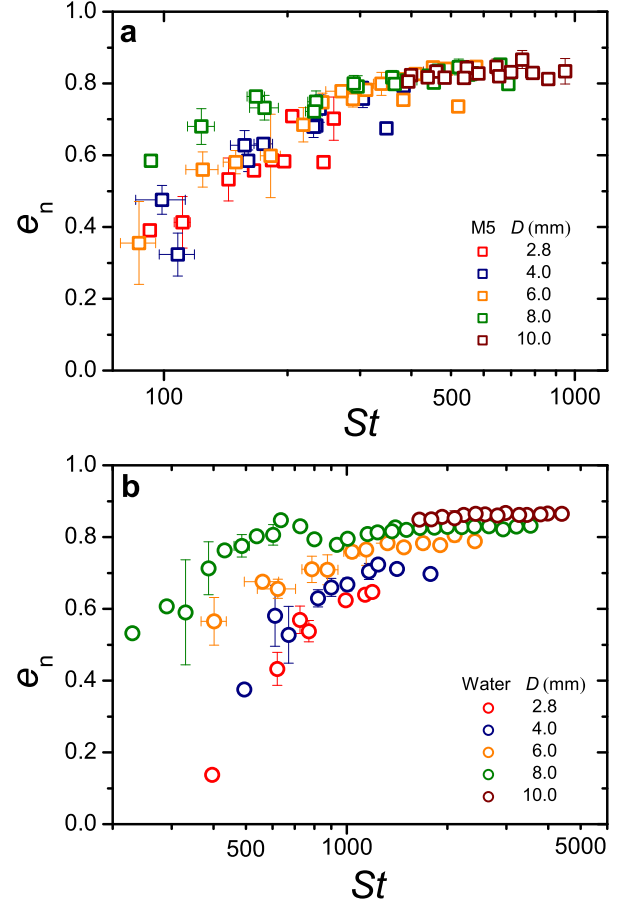


FIG. 6. (color online) Normal restitution coefficient e_n as a function of the Stokes number St for both silicone oil (a) and water (b) films. Parameters are the same as in Fig. 4.

more than an order of magnitude larger than that for M5, within the range of film thicknesses used. This suggests that E_c depends not only on the rupture energy of a capillary bridge, but also on viscous damping. As shown in Fig. 8(b), the slope e_{inf} is not strongly influenced by viscosity compared with E_c . For relatively thin film wetting, e_n could be the same within the error bars. The slope e_{inf} stays constant within the range of film thickness and decays slightly for more viscous M50 wetting.

Since the influence of the viscosity could be characterized by the Stokes number, we replot e_n , now as a function of St . As shown in Fig. 9(a), the COR grows dramatically at small St , which corresponds to the data of the M50 wetting case, and saturates at larger St . For various film thickness δ , this trend is qualitatively the same. Quantitatively, the saturated value e_{inf} decreases as δ grows, indicating that the assumption of small dimensionless film thickness δ/D for the lubrication theory to apply could not be fulfilled for the whole range of St investigated here. In other words, this feature shows that a further dimensionless parameter including the film thickness should be considered beyond the viscous dominating

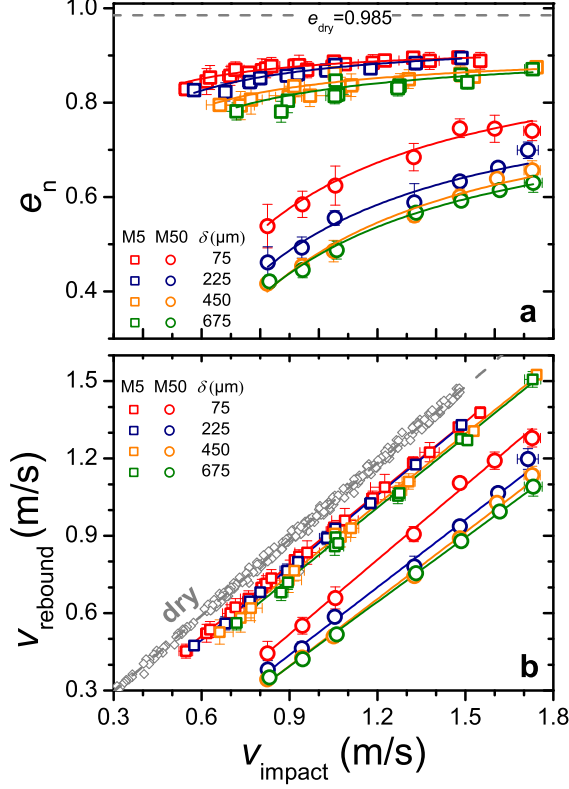


FIG. 7. (color online) The normal restitution coefficient e_n (a) and rebound velocity v_{rebound} (b) as a function of impact velocity v_{impact} for impacts of a glass bead with $D = 5.5$ mm on dry and wet surfaces covered with silicone oil M5 and M50. δ denotes the film thickness. The error bars correspond to the statistical error over 10 runs of experiments for the wet impacts. Solid lines in (b) are linear fits to the corresponding data. Their representatives are shown in (a) as a guide to the eye. Squares and dots correspond to M5 and M50, respectively. For dry impacts, the restitution coefficient e_{dry} is 0.985 with an error of 0.001.

regime.

This parameter is chosen as the dimensionless length scale $\tilde{\delta} = \delta/D$, because it ties the Stokes number with the Reynolds number of the wetting liquid. According to this definition, the ratio between the Reynolds number and the Stokes number is $Re/St = 9\tilde{\delta}\tilde{\rho}$, where $\tilde{\rho} = \rho_l/\rho_g$ is the density ratio between the liquid and the particle.

In Fig. 9(b), further experiments with the restriction $\tilde{\delta} \approx 0.04$ are presented. In contrast to Fig. 9(a), the data from various film thicknesses coincide over a wide range of St if $\tilde{\delta}$ is fixed. It also gives rise to a master curve $e_n = e_{\text{inf}}(1 - St_c/St)$, as indicated clearly in the inset. The linear fit yields $e_{\text{inf}} = 0.908 \pm 0.002$, and a critical Stokes number $St_c = 14.00 \pm 0.20$. Therefore, the usage of the Stokes number as a control parameter could be extended to the regime $Re > 1$ and large film thickness, provided that the dimensionless length scale $\tilde{\delta}$ is kept constant.

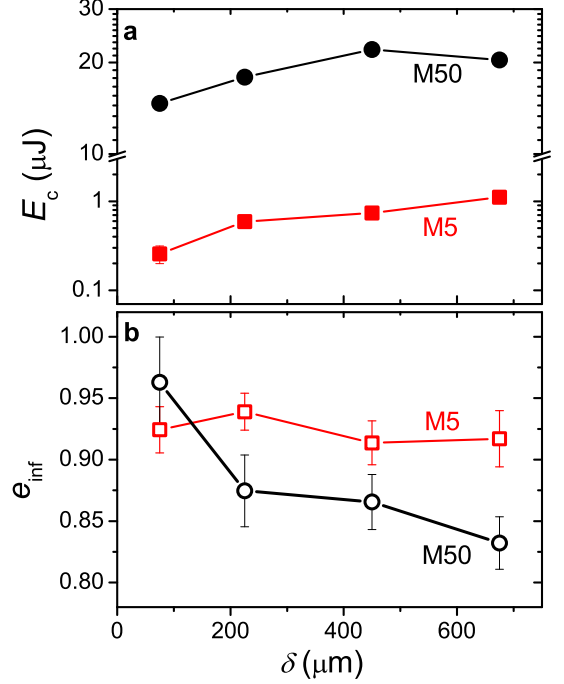


FIG. 8. The critical energy E_c and the saturated value of the COR e_{inf} as a function of the film thickness δ . E_c is obtained from the intersection v_c of the linear fits shown in the lower panel of Fig. 7 with the x-axis. e_{inf} corresponds to the slope of these fits.

IV. ANALYSIS OF THE ENERGY DISSIPATION

To understand the dependence of the COR on various particle as well as liquid properties, it is helpful to analyze the associated energy dissipation. With E_{diss} being the total kinetic energy loss of the particle during the impact, the dependence of the COR on the kinetic energy at impact E_i can be written as

$$e_n = \sqrt{1 - E_{\text{diss}}/E_i}. \quad (1)$$

The dissipated energy E_{diss} can be treated as the sum of two parts: the part transferred into the solid body ΔE_{dry} , and the other part taken by the wetting liquid ΔE_{wet} , i.e.

$$E_{\text{diss}} = \Delta E_{\text{dry}} + \Delta E_{\text{wet}}. \quad (2)$$

Provided that the two parts are independent from each other, i.e. the wetting liquid does not change the energy dissipation of the dry impact, ΔE_{wet} could be obtained experimentally by

$$\Delta E_{\text{wet}} = E_i(e_{\text{dry}}^2 - e_n^2). \quad (3)$$

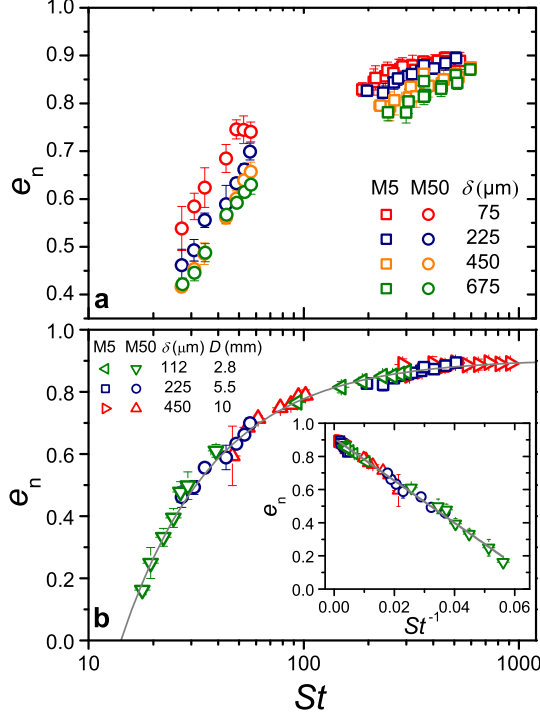


FIG. 9. (color online) The normal restitution coefficient as a function of the Stokes number St . (a) corresponds to the data shown in Fig. 7. (b) corresponds to the data with the dimensionless film thickness δ/D roughly constant. The error bars correspond to the statistical error of 10 runs of experiments. The solid curve in (b) corresponds to the master curve $e_n = 0.908(1 - 14.00/St)$, which is obtained from a linear fit to all the data shown in the inset.

The whole process of the colliding event can be separated into two parts: impact and rebound. During the impact, the kinetic energy of the particle will partly be transferred to the wetting liquid. This amount of energy will finally be dissipated by the motion of the viscous liquid, including surface waves or even splashes, depending on the competition between the inertial, viscous and surface forces. During the rebound, the rupture of the capillary bridge will lead to a certain amount of surface energy loss in addition to the damping caused by the motion of the liquid. Moreover, the mass of the wetting liquid dragged away by the sphere might lead to a further reduction of the COR. Based on the above analysis, one can take the most prominent terms and use

$$\Delta E_{\text{wet}} \approx \Delta E_{\text{visc}} + \Delta E_b + \Delta E_{\text{acc}} \quad (4)$$

to estimate ΔE_{wet} theoretically, where ΔE_{visc} represents the energy dissipated via the viscous damping force acting on the particle, ΔE_b corresponds to the energy loss arising from the surface energy change of the fluid, and ΔE_{acc} is the kinetic energy change of the fluid before and

after the colliding event.

In the limit that the thin film lubrication theory applies, the viscous force acting on the particle can be estimated by $F_v = 3\pi\eta D^2 v_{\text{impact}}/2x$ [33], where x denotes the distance between the sphere and the plate. Following Ref. [21], one might assume the same force law for both approach and departure of the sphere. By integrating over the distance that the viscous force applies, we obtain

$$\Delta E_{\text{visc}} = \frac{3}{2}\pi\eta D^2 v_{\text{impact}} \left(\ln \frac{\delta}{\epsilon} + \ln \frac{\delta_r}{\epsilon} \right), \quad (5)$$

where $\epsilon = 5 \mu\text{m}$ is the roughness of the sphere, and δ_r is the rupture distance of the liquid bridge. For a crude estimation, we take a fixed $\delta_r = 2D$ according to the snapshots taken and assume that the velocity does not change during the impact.

In Fig. 10, ΔE_{wet} for the experimental results shown in Fig. 7 is plotted in comparison with ΔE_{visc} . Qualitatively, the monotonic growth of the energy dissipation with the impact velocity, and the increase of energy dissipation with the film thickness agree with the estimation from Eq. (5). However, quantitatively a comparison between the estimated viscous damping term ΔE_{visc} and ΔE_{wet} reveals that a substantial amount of the latter can be attributed to the viscous damping for the case of M50 wetting, while this term plays a much weaker role for the case of less viscous silicone oil M5 wetting. Obviously, the growth of the difference with increasing v_{impact} and decreasing viscosity represents a deviation from the limit that lubrication theory applies. Taking 30% deviation as the limit, one can estimate the corresponding Reynolds number to be $Re \approx 10$ for the case of $\tilde{\delta} \approx 0.04$. For M5 wetting, the growth of the energy dissipation ΔE_{wet} with v_{impact} deviates slightly from a straight line, suggesting that the dominating energy dissipation term has a higher order dependence on the impact velocity.

The second term in Eq. (4) stems from capillary forces. Upon rebound of the sphere, a liquid bridge may form between the sphere and the liquid surface. The corresponding energy dissipation due to the deformation and rupture of this liquid bridge can be estimated by an integration of the force arising from the surface tension over the length that it acts. This capillary force has two components: the surface tension acting on the perimeter of the neck ($2\pi r_n \gamma$ with r_n the neck radius and γ the surface tension), and the second part arising from the Laplace pressure p_b that acts on the cross-section of the neck ($-\Delta p_b \pi r_n^2$). Based on quasi-static experimental verifications, a close form approximation of the capillary force F_c between two spheres has been given as

$$F_c = \frac{\pi D \gamma \cos(\phi)}{1 + 2.1S^* + 10S^{*2}}, \quad (6)$$

where $S^* = s\sqrt{D/2V_b}$ is the half separating distance s rescaled by the characteristic length scale $\sqrt{D/2V_b}$ with

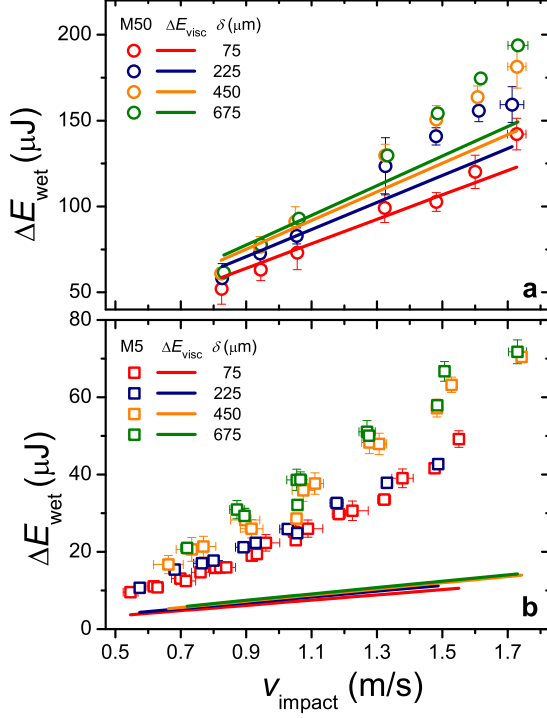


FIG. 10. (color online) Energy dissipation ΔE_{wet} due to wetting as a function of impact velocity with the wetting liquid properties the same as in Fig.7 for both silicone oil M50 (a) and M5 (b) wetting. Solid lines represent estimated values of the energy dissipation ΔE_{visc} from viscosity (see text for detailed descriptions). The line colors are in accordance with the data points for various film thickness.

the bridge volume V_b , and ϕ corresponds to the contact angle [44].

Taking the rupture distance δ_c as the integration limit, one could estimate the rupture energy of the liquid bridge to be

$$\Delta E_b \approx \pi \gamma \sqrt{2V_b D}. \quad (7)$$

A rough estimation of the bridge volume $V_b \approx D^3/16$, based on the snapshot taken, gives rise to $E_b \approx 0.7 \mu\text{J}$ for silicone oil wetting a glass bead with diameter 5.5 mm. Considering the energy dissipation obtained by the COR measurements shown in Fig. 10, E_b plays a minor role for the few mm sized particle used here. Note that E_b plays a more prominent role as D decreases, because its growth with \sqrt{D} is in contrast to $E_{\text{visc}} \propto D^2$.

As demonstrated in Fig.10, both the damping from the viscous force and the rupture of liquid bridges can not explain the amount of energy dissipation for the case of silicone oil M5 wetting. Therefore, other effects, like e.g. the inertia of the liquid or surface waves, should be considered.

As a first approximation, the inertial effect could be

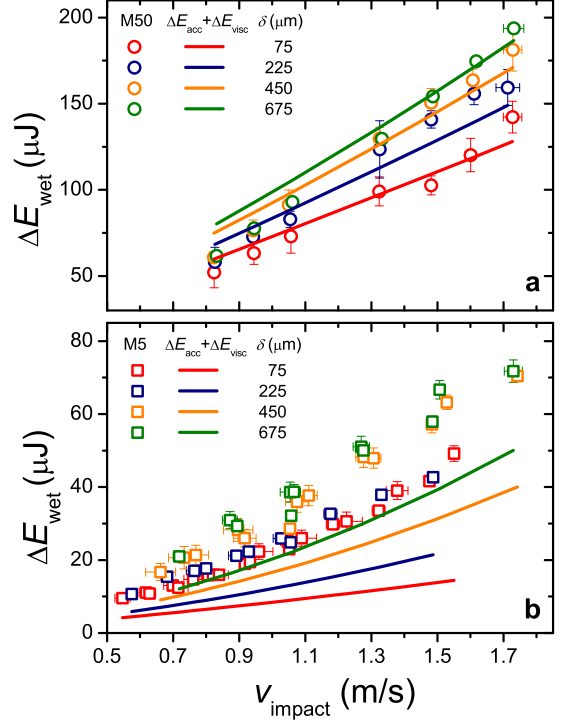


FIG. 11. (color online) Data points are the same as shown in Fig.10. Solid lines represent estimated values with the consideration of both viscous damping ΔE_{visc} and the energy transfer to the fluid ΔE_{acc} (see text for detailed descriptions). The line colors are in accordance with the data points for various film thickness.

estimated from the kinetic energy of the liquid being pushed aside by the impact [45]. The volume of the liquid can be estimated by the spherical cap immersed in the liquid film $V = \pi D^3 \tilde{\delta}^2 (1/2 - \tilde{\delta}/3)$. From the length scale taken as the base radius of the spherical cap $\sqrt{1 - (1 - 2\tilde{\delta})^2 D/2}$ and the time scale δ/v_{impact} for the particle to penetrate the liquid layer, one estimates the average velocity $v_l = v_{\text{impact}} \sqrt{1/\tilde{\delta} - 1}$. As a consequence, the kinetic energy ΔE_{acc} of the liquid being pushed aside yields

$$\Delta E_{\text{acc}} = \frac{1}{2} \rho_l V v_l^2 = 3\tilde{\rho} \left(\tilde{\delta} - \frac{5}{3} \tilde{\delta}^2 + \frac{2}{3} \tilde{\delta}^3 \right) E_i, \quad (8)$$

which shows a linear dependence on the kinetic energy E_i of the impact particle. Figure 11 shows that, by taking both ΔE_{visc} and ΔE_{acc} into account, the influence from the inertia effect is more prominent for less viscous M5 wetting. The combination of both forces leads to a better agreement with the experimental data, when compared to Fig.10(b). However, considering both the inertial and the viscous damping parts of the energy dissipation can not explain the experimental results for less viscous M5

wetting quantitatively. This indicates that further theoretical considerations, e.g. on additional energy dissipation terms, or a more careful characterization of the inertial effects, are desirable.

The fact that the ratio between ΔE_{acc} and E_i is not velocity dependent suggests that the inertia of the wetting liquid will not contribute to the impact velocity dependence of the e_n . It does, however, explain why e_{inf} obtained from linear fits of the data is generally smaller than e_{dry} . Based on the Eqs. (3) and (4), the E_i dependent COR could be written as

$$e_n = \sqrt{e_{\text{dry}}^2 - \frac{\Delta E_{\text{acc}}}{E_i} - \frac{\Delta E_{\text{visc}}}{E_i} - \frac{\Delta E_b}{E_i}}. \quad (9)$$

In the limit of large v_{impact} , the last term $\Delta E_b/E_i$ could be safely ignored so that two independent parameters are enough to determine the impact velocity dependence of the COR. A comparison to the linear fits $e_n = e_{\text{inf}}(v_{\text{impact}} - v_c)$ employed before immediately reveals that the linear fit is a first order approximation of the Eq. (9) and $e_{\text{inf}} = \sqrt{e_{\text{dry}}^2 - \Delta E_{\text{acc}}/E_i}$. By ignoring the higher order terms of $\tilde{\delta}$ in ΔE_{acc} , one derives a linearized form $e_{\text{inf}} = e_{\text{dry}} - 3\tilde{\rho}\tilde{\delta}/2e_{\text{dry}}$, which suggests a reduction of e_{inf} from e_{dry} by about 0.06 for typical experimental values of $\tilde{\rho} = 1/2.5$ and $\tilde{\delta} = 0.1$. A comparison to Fig. 8(b) shows that this simplified formula gives the correct order of magnitude for the e_{inf} estimation. Moreover, the monotonic decrease with $\tilde{\delta}$ is captured by this formula qualitatively, except for the 75 μm thick M5 wetting case.

V. CONCLUSION

In summary, the normal coefficient of restitution (COR) for a free falling sphere on a wet surface is investigated experimentally. The dependence of the COR on the impact velocity and various particle and liquid film properties is discussed in relation to the energy dissipation associated with the impact process.

i) For dry impact, the COR corresponds to the slope of the rebound vs. impact velocity. For wet impacts, the rebound velocity and the impact velocity are also found to fall into a straight line, but with a smaller slope and an offset corresponding to a finite critical impact velocity. Even though linear fitting is only a first order approximation of e_n , it successfully characterizes the impact velocity dependence of the COR with two parameters e_{inf} and E_c . Therefore this simplification is justified to be a good candidate for computer simulations aiming at modeling wet granular dynamics on a large scale.

ii) The dependence of the COR on the impact velocity, dimension of the sphere and the viscosity of the liquid could be well characterized by the Stokes number, which is defined as the ratio between the inertia of the sphere and the viscosity of the liquid, provided that the dimensionless length scale $\tilde{\delta}$ is fixed. This result supports the usage of the Stokes number for scaling the data, even beyond the low Reynolds number regime where it has originally been introduced.

iii) Concerning the energy dissipation arising from the wetting liquid, the viscous damping term dominates for Reynolds number up to $Re \approx 10$. Away from that limit, further effects, such as the inertia of the liquid film, have to be considered. The rupture energy of a capillary bridge during the rebound process could be safely ignored for the few mm sized particles used here.

The authors would like to acknowledge Mario Schörner for the help in the construction and calibration of the film thickness measurement part of the setup, and Bryan J. Ennis and Jürgen Vollmer for helpful hints. This work is partly supported by the German Science Foundation within Forschergruppe 608 ‘Nichtlineare Dynamik komplexer Kontinua’ through Grant No. Kr1877/3-1.

-
- [1] I. Newton, *Mathematical Principles of Natural Philosophy* (1687) Axioms, or Laws of motion. Corollary VI.
 - [2] H. Hertz, *J. reine und angewandte Mathematik* **92**, 156 (1882).
 - [3] A. E. H. Love, *A Treatise on the Mathematical Theory of Elasticity* (Dover, 1927).
 - [4] R. Ramírez, T. Pöschel, N. V. Brilliantov, and T. Schwager, *Phys. Rev. E* **60**, 4465 (1999).
 - [5] D. Tabor, *Proc. R. Soc. London* **192**, 247 (1948).
 - [6] K. L. Johnson, *Contact Mechanics* (Cambridge University Press, 1985).
 - [7] H. M. Jaeger, S. R. Nagel, and R. P. Behringer, *Rev. Mod. Phys.* **68**, 1259 (1996).
 - [8] J. Duran, *Sands, Powders and Grains (An Introduction to the Physics of Granular Materials)*, 1st ed. (Springer-Verlag, New York, 2000).
 - [9] S. L. Masami Nakagawa, ed., *Proceedings of The 6th International Conference on Micromechanics of Granular Media* (2009).
 - [10] N. V. Brilliantov, F. Spahn, J.-M. Hertzsch, and T. Pöschel, *Phys. Rev. E* **53**, 5382 (1996).
 - [11] N. Brilliantov and T. Pöschel, *Kinetic theory of granular gases* (Oxford Univ. Press, 2004).
 - [12] J. T. Jenkins and S. B. Savage, *J. Fluid Mech.* **130**, 187 (1983).
 - [13] I. Goldhirsch, *Annu. Rev. Fluid Mech.* **35**, 267 (2003).

- [14] F. Spahn and J. Schmidt, *GAMM-Mitt.* **29**, 115 (2006).
- [15] C. Bizon, M. D. Shattuck, J. B. Swift, W. D. McCormick, and H. L. Swinney, *Phys. Rev. Lett.* **80**, 57 (1998).
- [16] S. Herminghaus, *Adv. Phys.* **54**, 221 (2005).
- [17] P. Jop, Y. Forterre, and O. Pouliquen, *Nature* **441**, 727 (2006).
- [18] H. Rumpf, *Agglomeration* (AIME, Interscience, New York, 1962).
- [19] W. B. Pietsch, *Nature* **217**, 736 (1968).
- [20] B. J. Ennis, J. L. Li, G. Tardos, and R. Pfeffer, *Chemical Engineering Science* **45**, 3071 (1990).
- [21] B. J. Ennis, G. Tardos, and R. Pfeffer, *Powd. Technol.* **65**, 257 (1991),.
- [22] S. Iveson, J. Litster, and B. Ennis, *Powder technology* **88**, 15 (1996).
- [23] S. M. Iveson and J. D. Litster, *Powd. Technol.* **99**, 234 (1998).
- [24] S. M. Iveson, J. D. Litster, K. Hapgood, and B. J. Ennis, *Powd. Technol.* **117**, 3 (2001).
- [25] J. Fu, M. J. Adams, G. K. Reynolds, A. D. Salman, and M. J. Hounslow, *Powder Technology* **140**, 248 (2004).
- [26] S. Antonyuk, S. Heinrich, N. Deen, and H. Kuipers, *Particuology* **7**, 245 (2009).
- [27] P. Müller, S. Antonyuk, M. Stasiak, J. Tomas, and S. Heinrich, *Granular Matter* **13**, 455 (2011).
- [28] D. N. Mazzone, G. I. Tardos, and R. Pfeffer, *Powder technology* **51**, 71 (1987).
- [29] K. Murase, T. Mochida, and H. Sugama, *Granular Matter* **6**, 111 (2004).
- [30] R. Davis, J.-M. Serayssol, and E. J. Hinch, *J. Fluid Mech.* **163**, 479 (1986).
- [31] G. Barnocky and R. H. Davis, *Phys. Fluids* **31**, 1324 (1988).
- [32] C. Thornton and Z. Ning, *Powder Technology* **99**, 154 (1998).
- [33] R. H. Davis, D. A. Rager, and B. T. Good, *J. Fluid Mech.* **468**, 107 (2002).
- [34] A. A. Kantak and R. H. Davis, *Powd. Technol.* **168**, 42 (2006).
- [35] C. M. Donahue, C. M. Hrenya, and R. H. Davis, *Phys. Rev. Lett.* **105**, 034501 (2010).
- [36] C. M. Donahue, C. M. Hrenya, R. H. Davis, K. J. Nakagawa, A. P. Zelinskaya, and G. G. Joseph, *Journal of Fluid Mechanics* **650**, 479 (2010).
- [37] S. Ulrich, T. Aspelmeier, A. Zippelius, K. Roeller, A. Fingerle, and S. Herminghaus, *Phys. Rev. E* **80**, 031306 (2009).
- [38] A. Fingerle, K. Röller, K. Huang, and S. Herminghaus, *New J. Phys.* **10**, 053020 (2008).
- [39] A. Fingerle and S. Herminghaus, (2008), [arXiv:0708.2597](https://arxiv.org/abs/0708.2597).
- [40] Y. Couder, S. Protiere, E. Fort, and A. Boudaoud, *Nature* **437**, 208 (2005).
- [41] F. Blanchette and T. Bigioni, *Nature physics* **2**, 254 (2006).
- [42] C. Kimme, D. Ballard, and J. Sklansky, *Commun. ACM* **18** (1975).
- [43] M. Montaine, M. Heckel, C. Kruelle, T. Schwager, and T. Poschel, *Phys. Rev. E* **84**, 041306 (2011).
- [44] C. Willett, *Langmuir* **16**, 9396 (2000).
- [45] Jürgen Vollmer, private communications.